Accumulation of short-, medium-, and long- chain chlorinated paraffins in tissues of laying hens after dietary exposure

Marie Mézière[1], Philippe Marchand[1], Frédéric Larvor[1], Elisabeth Baéza-Campone[2], Bruno Le Bizec[1], Gaud Dervilly[1], Ronan Cariou[1,*]

[1]*LABERCA, Oniris, INRAE, 44307, Nantes, France.*

[2]*INRAE, Université de Tours, BOA, 37380 Nouzilly, France*

*Corresponding author at: Laboratoire d'Étude des Résidus et Contaminants dans les Aliments (LABERCA), Oniris, Route de Gachet, Nantes, F-44307, France

E-mail address: laberca@oniris-nantes.fr

Abstract

Reliable human health risk assessment associated with chlorinated paraffins (CPs) exposure is limited by the lack of data on the fate of this complex family of contaminants. To gain knowledge on the accumulation and distribution of CPs in biota after ingestion, laying hens were dietary exposed to technical mixtures of short- (SCCPs), medium- (MCCPs), or long-chain (LCCPs) CPs of various chlorine contents during 91 days, at 200 ng/g of feed, each. Adipose tissue, liver, muscle and serum were collected at the steady-state, along with excreta. All C_{10}-C_{36} CPs were detected in liver. However, differences were observed in CP distribution: LCCPs high %Cl were retained in the liver; LCCPs low %Cl circulated through the serum and were distributed in the different compartments, but were mostly excreted through the eggs; SCCPs and MCCPs were found in all tissues at similar levels. Finally, a mass balance indicated a potential for biotransformation.

Keywords (*6 max*)

chlorinated paraffins; homologue; distribution; accumulation ratio; dietary exposure; persistent organic pollutant

1. Introduction

Chlorinated paraffins (CPs), a family of polychlorinated *n*-alkane chains ($C_xH_{2x+2-y}Cl_y$) with varying chain length and chlorination degrees in the range 30-70% *w/w*, have been used since the late 1970s in many industrial applications such as lubricants in metal-working fluids, flame-retardants and plasticisers (European Food Safety Authority (EFSA) panel on contaminants in the food chain (CONTAM), 2020). Consequently, CPs are produced in large volumes (estimated at 1,000,000 tonnes per year, Glüge et al., 2016). Unfortunately, part of those CPs are released during production, uses and improper disposal of polymeric products containing these additives (Glüge et al., 2016). Thus, the CPs environmental levels usually surpass most of the levels of other halogenated contaminants such as polychlorobiphenyls, organochlorine pesticides or dioxins (Zhou et al., 2018; Krätschmer et al., 2019; Niu et al., 2020). CPs have been reported in most environmental compartments, such as air (Niu et al., 2020), water (X.-T. Wang et al., 2019), soil (Aamir et al., 2019), sediment (Chen et al., 2011), biota (Yuan et al., 2019), food (Harada et al., 2011; Lee et al., 2020) and even human matrices (Y. Wang et al., 2018). The ubiquity of CPs in the environment make them chemicals of concern, notably because they share similar physio-chemical properties with other halogenated contaminants that are considered hazardous for human health.

CPs are sub-categorised into short-chain CPs (SCCPs, C_{10}-C_{13}), medium-chain CPs (MCCPs, C_{14}-C_{17}), and long-chain CPs (LCCPs, $C_{\geq 18}$). SCCPs were classified as possibly carcinogenic to humans in 1990 by the International Agency for Research on Cancer (IARC working Group on the Evaluation of Carcinogenic Risk to Humans, 1990), and were later shown to cause chronic toxicity to marine species and mammals (X. Wang et al., 2019). As a consequence, they have been phased out in Europe and North America (European Union, 2006; Government of Canada, 2009; United States Environmental Protection Agency (US EPA), 2015) since the 2010s and included in the Annex A of the Stockholm convention in 2017 (Conference of the Parties of the Stockholm Convention, 2017). However, there is a lack of toxicity and toxicokinetics data on MCCPs and LCCPs, though recent occurrence studies on terrestrial and marine ecosystems show their potential for bioaccumulation (Yuan et al., 2019). Recently, the EFSA published

58 a scientific opinion on CPs concluding that risk assessment in Europe was hardly feasible, based on the
59 few submitted toxicological and occurrence data (EFSA CONTAM panel, 2020) at the time of their
60 evaluation. In particular, they emphasised the need for further information on the influence of the
61 chain length and the chlorination degree of CPs on their toxicokinetics in humans and experimental
62 animals.
63 To date, the few published toxicokinetics experiments focused on SCCPs and MCCPs mainly. In rodents,
64 ^{14}C-labelled SCCPs have been reported to be distributed primarily in fat, liver, bile and egg yolks
65 (Biessmann et al., 1982, 1983). The authors also showed that lower chlorinated compounds could
66 undergo degradation to CO_2, whereas the higher chlorinated compounds could not. Later, Fisk et al.
67 (1998) showed accumulation of SCCPs and MCCPs congeners in dietary exposed rainbow trout. In their
68 study, the depuration half-lives varied from 5 to 53 days depending on the octanol-water partition
69 coefficient (K_{ow}) and carbon chain length, indicating an influence of the homologue structure on the
70 accumulation potential. More recently, Geng et al. (2016) observed SCCPs absorption and depuration
71 in rats after a single-dose exposure. Alike other persistent organic pollutants, SCCPs distributed in
72 tissues sensitive to the chlorine content. These studies demonstrated well the influence of the
73 homologue structure on the bioaccumulation but were limited to C_{10}-C_{14} chain lengths. In parallel, one
74 study on SCCPs, MCCPs, and LCCPs in exposed aquatic invertebrates *via* contaminated water and feed
75 revealed the strong potential of LCCPs for accumulation (Castro et al., 2019). However, contaminants
76 have been shown to feature diverse accumulation behaviours in aquatic or terrestrial species (Sun et
77 al., 2017). It was therefore of particular interest to extend the knowledge on the toxicokinetics of
78 SCCPs, MCCPs and LCCPs at a homologue level on terrestrial vertebrates.
79 In the present study, the laying hen was selected as model organism, as it is a widely distributed farmed
80 animal around the globe. Two previous experiments on hens confirmed the accumulation of SCCPs in
81 abdominal fat, liver and kidney, although the relative concentration in the tissues did not follow the
82 same trends (Ueberschär et al., 2007; Sun et al., 2017). In a previous work (Mézière et al., 2021), we
83 exposed laying hens to an exposure mixture of CPs with various chain lengths and chlorination degrees,

at environmentally relevant levels (5×200 ng/g ww, Dong et al., 2019). Substantial amounts of CPs were found in eggs, suggesting that CPs could be absorbed and distributed in laying hens. In this study, we hypothesised that this distribution would be dependent on the homologue formula. We thus collected various tissues and fluids (muscle, liver, fat, serum, and the rest of the carcass) at days 77 and 91, days at which we believed the steady-state was reached. Additionally, excreta (faeces + urine) was collected to attempt a mass balance. The results provide valuable data on bio availability and distribution of CPs in the hens. In particular, to our knowledge this is the first time that LCCPs fate in terrestrial birds has been reported.

2. Material and methods

2.1. Chemicals

The chemicals used in this study, including the five CP technical mixtures for feed fortification, internal and external standards, and other chemicals and solvents used during the sample preparation are detailed in the supplementary data (Section S1) and are the same as in our previous study (Mézière et al., 2021). The five CP technical mixtures cover a range of chain lengths and chlorine contents: SCCPs low %Cl (Chlorowax™ 500C SCCPs, low chlorine content), SCCPs high %Cl (Paroil™ 179 HV, SCCP, high chlorine content), MCCPs (I-42, low chlorine content), LCCPs low %Cl (Unichlor™ 40-90, LCCP, low chlorine content) and LCCPs high %Cl (CPW 100, LCCP, high chlorine content) (Figure S1).

2.2. Feed, experimental design and sampling

The present work completes a kinetic study on CPs transfer to eggs of laying hens; details of feed and experimental design have been described previously (Mézière et al., 2021).

Briefly, a feed basis containing all required nutrients for laying hens was pelleted with non-spiked or spiked rapeseed oil (Table S1), for control and exposed groups respectively, with a target concentration in spiked feed of 200 ng/g ww for each of the five technical mixtures cited above (§2.1).

The animal experiment was ethically approved by the French authorities under number APAFIS#17145-2018101712299769v2 and was conducted in an appropriate facility (https://doi.org/10.15454/1.5572326250887292E12). After a one-month acclimation in individual cages, 25-week old laying hens (Isa Brown) were randomly separated into control and exposed groups (day 0) (Figure S2a). The control (n=6) and exposed (n=13) hens of interest for the present work weighed 1656 ± 81 g at day 0. They were fed with the corresponding feed (spiked or non-spiked) during 91 days. Feed intake was recorded weekly, by weighing feed allowance and refusals. Both groups ingested 110 ± 12 g daily of feed along the experiment.

Hens were weighed and slaughtered after a 12 h fast, on day 77 (5 exposed) or day 91 (6 controls and 8 exposed), by electrical stunning followed by carotid artery section. Blood was collected and serum separated after coagulation. Then, hens were plucked and the liver, abdominal fat and muscles of the left leg (thigh and drumstick) were collected and weighed. The rest of the carcass (blood clot included) was weighed and kept as well. In addition, the excreta (faeces + urine) produced during the last 14 days of individuals slaughtered at day 91 were collected and mixed. All samples were stored at -20 °C until analysis.

2.3. Extraction and Clean-up

Carcasses were ground and homogenised in an appropriate facility. Then, carcasses, livers and muscles were lyophilised. Excreta were dried in oven at 60 °C during 2 days (Figure S2b).

CPs were co-extracted with lipids from 1.5, 2, 5 and 1 g of dry carcass, liver, muscle and excreta, respectively, using pressurised liquid extraction (SpeedExtractor E-914/E-916, Büchi, France) with a mixture of toluene/acetone (7:3, *v/v*, 3 static cycles, 120 °C, 100 bar). For adipose tissue, 0.5 g of liquid fat was directly aliquoted. ^{13}C-γ-Hexabromocyclododecane (^{13}C-γ-HBCDD, 5 ng) was added to lipidic extracts as internal standard, and fat contents were determined gravimetrically. Serum (10 g) was extracted by liquid-liquid extraction after adding the internal standard. Proteins were precipitated with dipotassium oxalate, and extraction was performed with two cycles of methanol-diethyl ether-

135 petroleum ether mixtures and decantation. The two organic phases were filtered and reassembled.
136 Lipid classes (triglycerides, esterified and free cholesterol, phospholipids) in serum were determined
137 according to 4 enzymatic kits (Biolabo, Maizy, France) (Marchand et al., 2010) and the total lipid
138 content was then calculated as their sum.
139 Lipidic extracts were purified according to Mézière et al. (2021) using packed columns containing acidic
140 silica gel and deactivated Florisil. The extracts were reconstituted in 25 µL of acetonitrile containing
141 d_{18}-β-HBCDD (0.2 ng/µL) as external standard.
142
143 *2.4. Data acquisition and data-treatment*
144 The instrumental set-up was identical to that of Mézière, Cariou, et al. (2020) and Mézière et al. (2021).
145 In short, sample extracts were analysed by reverse phase liquid chromatography-high resolution mass
146 spectrometry fitted with an electrospray ionisation source. A dichloromethane/acetonitrile mixture
147 (1:1, *v/v*) was added post-column to enhance the formation of the monitored $[M + Cl]^-$ adduct ions,
148 from $C_{10}Cl_4$ to $C_{36}Cl_{30}$. Corresponding signals were extracted (±5 ppm) and integrated using the open
149 source programming *R* environment. After application of identification criteria (isotopic ratio and
150 minimum intensity), signals of the quantifier ions were normalised by their isotopic contributions.
151
152 *2.5 Quantification and accumulation calculations*
153 Quantification of the five CP subcategories studied (Figure S1) was performed by external calibration
154 similarly as in our previous work on eggs Mézière et al. (2021). A serial dilution (9 points) of the five
155 technical mixtures was performed within the dynamic range of 0.1-15 ng/µL for each technical mixture.
156 After control of the instrumental performances with the external standard, the areas of homologues
157 were summed per technical mixtures. Then, the ratio of CP sum area to the internal standard area was
158 correlated to the ratio of the corresponding technical mixture concentration to the internal standard
159 concentration. It should be noted that some homologues overlapped between the SCCPs and the
160 MCCPs (Figure S1, C_{13} to C_{15} homologues). However, since we used the same solutions for exposure

and quantification, the resulting calibration curves remain representative of the CPs in the samples, overlap included. The dynamic range was divided into two sub-ranges (0.5-2 and 2-15 ng/µL) which fitted adequately with linear curves.

The similarities between the CP homologue response patterns of the calibration solution and the tissues was assessed using a least-square approximation with a non-negative constraint (*lsqnonneg* function, *pracma* package, open source programming *R* environment). The profiles were considered as a good match when the parameter *a* of the equation $[S] = a \times [M] + b$ was close to 1 (± 0.1), where $[S]$ and $[M]$ are the vectors of the homologues detected in the sample and the corresponding technical mixture, respectively.

Considering that the steady-state was reached, the accumulation ratios ($AR_{CP\ subcat.}$) in the samples (S) could be calculated in exposed hens according to equation 1:

$$AR_{CP\ subcat.} = \frac{C_{CP\ subcat.}(S)}{C_{CP\ subcat..}(feed)} \quad \text{Eq.1}$$

where $C_{CP\ subcat.}(S)$ and $C_{CP\ subcat.}(feed)$ are the concentrations of the CP subcategories in the tissue (ng/g lw) and the spiked feed (ng/g ww), respectively.

The concentrations of each homologue in the technical mixture was not known, thus the homologue concentration could not be calculated. However, we followed that same reasoning as detailed in our previous work (Mézière et al., 2021) to calculate homologue-level accumulation ratios. Indeed, the concentration of a homologue n, x can be expressed according to the exposure mixture concentration at which the same homologue n, x would have the same relative intensity ($A_{n,x}/A_{IS}$) and the contribution of the homologue to this exposure mixture (although not known). As the spectrometric response of the homologue is considered to be the same in the tissues or the feed, this term can be eliminated from the equation and the accumulation ratio can be calculated using the ratio of areas of the homologue in the feed and in the tissues. The final expression can be written as follows:

$$AR^{S}_{n,x} = \frac{Q^{S}_{IS}}{Q^{feed}_{IS}} \times \frac{SS^{feed}}{SS^{S}} \times \frac{f^{-1}_{n,x}\left(\frac{A^{S}_{n,x}}{A^{S}_{IS}}\right)}{f^{-1}_{n,x}\left(\frac{A^{feed}_{n,x}}{A^{feed}_{IS}}\right)} \quad \text{Eq. 2}$$

where $AR_{n,x}^{S}$ is the accumulation ratio of the homologue n,x, Q_{IS}^{S} and Q_{IS}^{feed} are the quantity of internal standard in the hen tissue or the feed, respectively, SS^{S} and SS^{feed} are the corresponding sample sizes, respectively, $f_{n,x}^{-1}$ corresponds to the calibration curve of the exposure mixture solutions, and $A_{n,x}^{S}$, A_{IS}^{S}, $A_{n,x}^{feed}$, A_{IS}^{feed} are the signal areas of the homologue n,x or the internal standard (IS) in the tissue (S) or the feed, respectively.

The $A_{n,x}^{S}$, could be calculated for each exposed individuals, respectively. Mean $A_{n,x}^{S}$ were calculated for homologues observed in at least 4 individuals (≥50% detection frequency) only.

2.6 QA/QC

All glassware was heated at 400 °C during 4 h before use. Tissues and excreta were prepared and analysed in distinct batches, along with a total of 25 procedural blanks and 20 quality control samples (QCs) when considering feed and egg yolk batches from the previous study as well. Traces of SCCPs low %Cl and MCCPs were found in all blank extracts at concentrations varying between 2-17 and 5-33 ng/sample, respectively (Table S2). Traces of LCCPs low %Cl were found as well in some batches at concentrations up to 32 ng/sample. Thus, homologue relative areas in samples were corrected from the corresponding homologue relative area in the blank prior to quantification. Recovery was evaluated during the previous study with a QC (mixture of exposed eggs from day 32 and day 88, spiked with LCCPs high %Cl at the level of 250 ng/g), and varied between 66% and 151% depending on the CP technical mixture. The variability intra-batch was considered acceptable (12-29%, Table S3). However, the inter-batch variability was slightly higher (26-41%), showing that there is still room for improving quantitative determination, although recent interlaboratory assays showed great progress on this matter (Krätschmer and Schächtele, 2019; Mézière, Krätschmer, et al., 2020). Method detection limits were not calculated (Mézière et al., 2021) and the limit of quantification (LOQ) was defined as the lowest point of the external calibration (0.1 ng/µL). This corresponded to 5 ng/g lw for adipose tissue, liver, muscle, carcass, to 25 ng/g lw for serum, and to 2.5 ng/g dw for excreta.

3. Results and discussion

The body weight of hens (day 77 and day 91) at slaughter did not significantly differ between the control (1646 ± 84 g) and the exposed (1661 ± 82 g) groups (P>0.1) (Table S4), nor between exposed hens slaughtered at day 77 or day 91 of the exposure. Additionally, the feed ingested daily was constant over time (P>0.1), and reached 66 ± 5 g/kg bw/day. Thus, all exposed hens were exposed to the same amount of CPs over the experiment.

As previously reported (Mézière et al., 2021), the control batch of the feed contained residues of SCCPs, MCCPs and LCCPs, likely originating from seed ingredients. Hence, the total exposure of the individuals considered in the present study corresponded to about 24, 26, 27, 22, and 34 µg/day of SCCPs low %Cl, SCCPs high %Cl, MCCPs, LCCPs low %Cl and LCCPs high %Cl, respectively.

3.1. CP mix level concentrations, AR and mass balance

3.1.1. Concentrations

Concentrations of CPs in the different tissues were constant between day 77 and day 91 of exposure (Figure S3), suggesting that the steady-state was reached before the end of the experiment. This is in line with the previously estimated time to reach the steady-state in eggs (~14 days, Mézière et al., 2021). For the following discussion, only concentrations calculated at day 91 are considered.

SCCPs and MCCPs were detected in all matrices, confirming that those CP subcategories permeated through the gastro-intestinal tract, transferred into blood and reached the different tissues (Figure 1, Table S5). In excreta, SCCPs low %Cl concentrations were lower than for the two other CP subcategories, suggesting a higher bioavailability compared to the other CP subcategories. SCCPs and MCCPs concentrations were relatively similar between the different matrices, although the muscle and serum appeared less contaminated and were close to or below the LOQ. This even distribution suggested that the distribution of SCCPs and MCCPs in different matrices may be driven mostly by hydrophobic interactions rather than more specific interactions (justifying a concentration reporting in lw). This is supported by previous experiments on SCCPs in laying hens and broilers (Ueberschär and

237 Matthes, 2004; Ueberschär et al., 2007) which also concluded in a lipid content-related accumulation
238 in tissues (fat > liver and yolk > muscle). Interestingly, SCCPs low %Cl were detected at lower levels
239 compared to SCCPs high %Cl and MCCPs. SCCPs with lower chlorine content have been shown to
240 degrade down to CO_2, whereas SCCPs high %Cl did not (Biessmann et al., 1982, 1983). The lower
241 concentration of SCCPs low %Cl may come from a higher potential for biodegradation compared to
242 CPs with higher Cl content and longer chains.
243 LCCPs low %Cl were also detected in all matrices, revealing their circulation in the hens. However,
244 concentrations were similar between the liver and serum, as well as in eggs (Mézière et al., 2021), but
245 were much lower in adipose tissue and muscle (Figure 1). This indicates a different mechanism of
246 distribution depending on the matrix for this type of CPs. It was already discussed for other
247 contaminants that the distribution is related to the perfusion rate of the tissues homologues (Pirard
248 and De Pauw, 2005), with compounds being firstly distributed into highly perfused matrices, and in a
249 second time reaching tissues of lower perfusion rate such as muscle and adipose tissue. Hence, it could
250 be hypothesised that with longer chain length, LCCPs reach the tissues of lower perfusion rate more
251 slowly than SCCPs and MCCPs, thus they preferentially accumulate in high perfusion matrices such as
252 eggs while SCCPs and MCCPs are readily accumulated homogeneously in the whole body. A slower
253 distribution of LCCPs may lead to a longer time to reach the steady-state. It would be interesting to
254 monitor the kinetics of CPs accumulation in tissues to investigate this hypothesis, although this was
255 not observed in eggs (Mézière et al., 2021).
256 Finally, LCCPs high %Cl were detected in a higher level in excreta compared to the other CP
257 subcategories, suggesting a more difficult absorption. If absorbed, they were detected in liver mostly,
258 with traces in eggs (Mézière et al., 2021) and serum (Figure 1). Such high concentration of LCCPs high
259 %Cl suggests that this CP subcategory can also reach the liver *via* the hepatic portal vein, supporting
260 their bioavailability. However, the low concentration in serum indicates that this CP subcategory is
261 retained in the liver or, alternatively, could be excreted *via* bile to the intestine from which it may be

excreted *via* the faeces or reabsorbed. This entero-hepatic cycle has been described for drugs in rats and dogs (Yesair et al., 1970). To support this hypothesis, analysis of the bile would be beneficial.

3.1.2. Accumulation ratios

Accumulation ratios (ARs) were estimated in each matrix using the mean concentrations of CP subcategories in exposed laying hen tissues (when <LOQ) and spiked feed (Table 1, Table S5). For all CP subcategories, ARs were higher for eggs, liver, and serum than for adipose tissue and muscle. This suggests that CPs are distributed preferably in liver and eggs compared to the inner tissues. Additionally, the ARs increased in the order SCCPs low %Cl < MCCPs < LCCPs and SCCPs low %Cl < SCCPs high %Cl for eggs, liver, and serum. ARs of the SCCPs high %Cl were compared with those previously reported by Ueberschär et al. (2007), where laying hens were dietary exposed to similar levels of SCCPs 60% Cl (140 ng/g ww feed) during 7 weeks, with a similar feed consumption (107-115 g/day). SCCPs accumulated more in abdominal fat (2.5 times) but less in eggs (2.5 times) compared to the present experiment. These differences could be explained by several hypotheses, including the influence of a different hen strain ("Lohmann selected leghom"), different chlorine content, and a cocktail effect arising from the simultaneous exposure to several mixtures in the present study.

Kan and Meijer (2007) proposed a classification of chlorinated pesticides according to the accumulation ratio. According to this basis, the CPs would be classified as low to moderately accumulative.

3.1.3. Mass balance

Considering that steady-state was reached in the carcass and sampled matrices by day 77 (Figure S3), a mass balance between CP input (feed, from Mézière et al., 2021) and monitored outputs (excreta, egg) was performed from day 77 to day 91. Average dried matter and lipid contents of samples are provided in Table S6.

Excreta released 0.8, 2.0, 1.9, 2.0, and 4.3 µg/day of SCCPs low %Cl, SCCPs high %Cl, MCCPs, LCCPs low %Cl and LCCPs high %Cl, respectively (Table S7), corresponding to 3%, 8%, 7%, 9%, and 13% of the ingested CP subcategories, respectively (Figure 2). Meanwhile, the egg yolks released 0.2, 0.8, 0.5, 7.0 and 0.13 µg/day of the five categories, corresponding to 1%, 3%, 2%, 32%, and 0% of the ingested CP subcategories, respectively. SCCPs low %Cl were the least released in the excreta at the steady-state, while the LCCPs high %Cl were the most released in the excreta, because of physical properties discussed earlier. Meanwhile, CPs proportion in eggs were lower compared to excreta, except for LCCPs low %Cl which featured high absorption but also a high transfer to eggs compared to SCCPs and MCCPs.

More importantly, the mass balances of CPs were underestimated from -59% for LCCPs low %Cl to -96% for SCCPs low %Cl (Figure 2, Table S7). Plausible unchecked excretion routes include feathers and preen oil, as observed for other contaminants (Rutkowska et al., 2018). Also, it should be noted that excreta were collected after 14 days. Thus, potential degradation of CPs in this time period from contact with microorganisms present in the excreta or air may also have impacted the mass balance.

However, we hypothesise that CPs are subjected to biotransformation. One recent study on *in vitro* enzymatic transformation with human liver microsomes showed a decreased of the CPs concentrations down to -97% depending on the enzyme used and CPs technical mixture (He, 2019). The authors suggested that CPs may degrade into shorter chain CPs, and observed the formation of CO-CPs products among four targeted biotransformation products. In our study, the CP response patterns did not shift towards shorter chain lengths, thus we considered that biotransformation products would be more plausible. Hence, we further explored the raw data acquired from egg, liver and carcass samples, using the post-acquisition data treatment software HaloSeeker 1.0 developed by Léon et al. (2019). Unfortunately, although CPs were clearly identified, no other polychlorinated series of signals could be observed in these high resolution mass spectrometry data sets. It should be however noted that the sample preparation was specifically developed for CPs, and biotransformation products may have been eliminated during one of the purification steps of the process. Further

313 characterisation of the CP metabolism should thus be performed in order to better apprehend the
314 mass balance of CPs in experimental animals, possibly with implementation of untargeted analytical
315 strategies from sample preparation to data treatment (Pourchet et al., 2020).
316
317 *3.2. Homologue response profile and homologue accumulation ratio*
318 3.2.1 Homologue response profiles
319 CPs bioavailability and accumulation were investigated more finely at the homologue level. First, CP
320 patterns between the various laying hen matrices and the exposure mixture were compared for the
321 exposed group (Figure 3) and control group (Figure S4). The surfaces of the CP patterns in the feed
322 matched closely the exposure mixture, confirming that the spiking was performed correctly. However,
323 shifts of the response patterns were observed in the matrices.
324 SCCPs and MCCPs were present in the 2D-map representations of every matrices and their surfaces
325 matched the one of the exposure mixture relatively well for excreta, liver, and carcass, but seemed
326 shifted towards higher chlorinated homologues in adipose tissue, serum and muscle. This shift was
327 discussed in our previous work on CPs in laying hens eggs, and was correlated to a homologue-
328 dependant accumulation ratio, caused by higher octanol-water partitioning coefficients (K_{ow}) (Mézière
329 et al., 2021). SCCPs low %Cl seemed lost in the 2D-representation of liver and serum, although they
330 were detected in both matrices. In liver, this is explained by the surface calculation which includes all
331 subcategories: the contribution of SCCPs low %Cl to the whole pattern of liver is too small compared
332 to the other subcategories. The predominance was marked by LCCPs low %Cl and LCCPs high %Cl. In
333 serum, SCCPs low %Cl were absent from the 2D-blank representation of the profiles after blank
334 subtraction.
335 LCCPs low %Cl surfaces underwent the same shift towards higher chlorinated homologues, but also
336 according to the chain length in the liver (C_{20} to $C_{>36}$). Oppositely, they were not represented in the 2D-
337 map of muscle and only shorter chain lengths were represented in adipose tissue (C_{20} to C_{30}). This
338 suggests that LCCPs low %Cl homologues are distributed differentially in the hens. The longest chain

lengths tended to be retained in the liver, similarly as for the LCCPs high %Cl technical mixture, while the shortest chain lengths were closer to the SCCPs/MCCPs behaviour.

Finally, most of the LCCPs high %Cl were observed in the liver and the excreta. In liver, only homologues up to $C_{30}Cl_{24}$ were detected, suggesting a that the longer/higher chlorinated homologues couldn't pass through the gastro-intestinal barrier. However, traces of the smallest homologues of this CP pattern were detected in serum and carcass, indicating that this CP subcategory should not be discarded too rapidly.

It should be noted that the quantification of the present study, based on external calibration using the exposure mixtures, was sensitive to the similarity of the response patterns between the tissues and the exposure mixture. Indeed, the instrumental response of the technical mixture was shown to be dependent on the overall chlorine content and chain length of the mixture (Mézière, Cariou, et al., 2020). This similarity was thus assessed to control the quantification accuracy by calculating a factor between the tissues and the exposure mixture that would be need to make the patterns match. In those conditions, a = 1 (± 0.1) would mean a perfect match, as demonstrated with the feed (Table 2). The best match was reached in the excreta. This was attributed to the release of a part of CPs into excreta directly without going through the gastro-intestinal tract, thus with only limited differentiation based on homologue structure and chemical properties. The weakest match was observed for SCCPs and MCCPs in the serum, which was attributed to undetected homologues on the fringe of the CP subcategory due to low levels in this matrix. For the other matrices, the least-square approximation returned medium values.

According to the non-negative least-square approximation results, quantification can be considered accurate for feed, excreta, adipose tissue, and carcass. It may however suffer more deviation to the true value for liver and muscle, and be considered as tentative only for SCCPs and MCCPs in serum.

Nevertheless, CP bioavailability and distribution in the hens was found homologue-dependant, which resulted in shifted response patterns compared to the exposure mixture. These results may help to refine the current knowledge on CPs fate in animals.

365

366 3.2.2 Homologue-level accumulation ratio

367 The accumulation ratios per homologue ($AR^{S}_{n,x}$, Eq. 3) were determined using the relative signal in
368 each considered matrix (n=8 individuals) and in the feed (mean of triplicate analysis). The mean and
369 uncertainty of $AR^{S}_{n,x}$ varied greatly, depending on the homologue and the tissue, from <1 to 103 for
370 the mean (Figure 4). The liver featured the highest accumulation ratios, which increased with chlorine
371 content and chain length up to an optimum reached for the $C_{32}Cl_{11}$ homologue (Figure 4). For a fixed
372 number of chlorines the highest $AR^{liver}_{n,x}$ were reached for 32 to 36 carbons in the chain, with the
373 optimum tending to decrease with increasing chlorine number (Table S8). For a fixed number of
374 carbon, optimums were reached for almost each chain length, with a broad range of chlorine numbers
375 (from $C_{18}Cl_9$ to $C_{27}Cl_{20}$). Interestingly, the $AR^{liver}_{n,x}$ of the LCCPs low %Cl homologues increased with the
376 chlorine content, while those of the LCCPs high %Cl homologue decreased. This strongly suggests that
377 optimums are reached for homologues in-between, which were not included in the exposure mixture.
378 $ARs^{serum}_{n,x}$ followed similar trends as in liver, i.e. a positive correlation between the $ARs^{serum}_{n,x}$ and the
379 chlorine number and chain length up to an optimum reached for $C_{32}Cl_{10}$. However, the values diverged
380 less ($ARs^{serum}_{n,x} =$ <0.1-13) and only three $ARs^{serum}_{n,x}$ could be calculated for LCCPs high %Cl with the
381 selected restriction (≥50% frequency) (Figure 4, Table S9). For a fixed number of chlorines, the
382 optimums were reached for shorter chain lengths (C_{26} to C_{32}) and tended to increase with increasing
383 chlorine content, oppositely to liver. For a fixed number of carbons, optimums were obtained for
384 homologues with Cl_9-Cl_{11}. Hence, liver retained more the higher chlorinated and of higher chain length
385 homologues. The trend obtained for the serum and the liver are close to the one obtained previously
386 for the eggs (Mézière et al., 2021), suggesting an important interaction between the three matrices.
387 The muscle and adipose tissues behaved differently. In the muscle, the $ARs^{muscle}_{n,x}$ did not increase
388 towards an optimum but rather formed a ridge in the direction of $C_{18}Cl_9$ to $C_{11}Cl_{11}$ (Figure 4, Table S10),
389 with lower accumulation ratios (0-8). This indicated that both chain length and chlorine content have
390 a positive influence on the accumulation ratio, but are hindered by another parameter such as the

molecular size, as the *m/z* of the homologues on the ridge are centred around 600. This is also supported by the rare $ARs_{n,x}^{muscle}$ calculated for LCCPs low %Cl, that highlighted the low detection frequency of this CP subcategory in muscle. Last, the $ARs_{n,x}^{adipose\ tissue}$ values were even lower and remained relatively stable (<0.1-0.9, Figure 4, Table S11), suggesting low accumulation in this tissue. Several maximums could be observed: one around $C_{12}Cl_{10}$, one around $C_{19}Cl_7$ and the other forming a ridge between $C_{26}Cl_5$ and $C_{30}Cl_9$. These lower accumulation ratios with distinct trends for muscle and adipose tissue suggest a different affinity of CPs for the inner organs of the laying hens compared to the liver, serum and eggs, that may take into account not only the CPs hydrophobic interactions but also specific interactions such as protein binding. To date, these specific CP interactions have been poorly studied and should be further investigated.

As previously discussed for LCCPs low %Cl (§3.1.1), it is not surprising that the liver, serum and eggs give similar results, as large flows of metabolites pass from the liver to the eggs via the bloodstream for a laying hen. On the other hand, in an adult hen, the growth of muscle and fat tissue is rather limited and there is little flow of metabolites, explaining the similar results for these two tissues.

To our knowledge, only three studies have reported CP dietary exposure of birds. Ueberschär and Matthes (2004) investigated SCCPs fate in broilers and Ueberschär et al. (2007) exposed laying hens to SCCPs, but neither articles discussed at the homologue level. Recently, Sun et al. (2020) reported SCCPs homologue accumulation ratios in close-range raised laying hens. Interestingly, the authors reported accumulation ratios decreasing with K_{ow}. We observed the opposite in our study, with homologue accumulation increasing with chain length and degree of chlorination, although the homologue log K_{ow} were not modelled here. However, many variables differed between the two experiments, notably the dietary exposure protocol (soil + feed, uncontrolled versus feed, controlled). Moreover, it should be noted that SCCPs K_{ow} varied between 5 and 6.6 in the study of Sun et al. (2020), whereas the K_{ow} range was larger in our study (up to ~12 for LCCPs). Thus, we believe that this study completes the current knowledge on homologue-level accumulation behaviour in birds.

4. Concluding remarks and perspectives

The present study aimed to provide a preliminary investigation on the distribution behaviour of CPs in exposed laying hens, depending on their chain length and chlorine number. The exposure of laying hens to five CPs technical mixtures of different chain lengths (SCCPs, MCCPs, LCCPs) and degree of chlorination (low versus high) enabled highlighting the bioavailability of all CP subcategories. However, striking differences according to the chain length and degree of chlorination were observed regarding their distribution in the laying hens. Up to a certain chain length and chlorination degree, CPs were released from the liver to the serum. However, some homologues (LCCPs high %Cl) were not at all detected in serum, suggesting either retention in liver or release through bile to the intestine. Analysis of this latter matrix would definitely complete the present study. The longest homologues of LCCPs low %Cl and the whole LCCPs high %Cl pattern were directly excreted in the eggs. Meanwhile, SCCPs, MCCPs, and the shortest homologues of the LCCPs low %Cl pattern could reach the internal tissues (muscle and adipose tissue). This observation confirmed the accumulation of SCCPs, and extended it to MCCPs and LCCPs. Additionally, the homologue-level accumulation ratio revealed similar behaviour of CPs in liver, serum and egg, but strong differences in the inner tissues. A depuration study that would provide half-lives for toxicokinetics considerations would complete the present work.

More importantly, this study revealed an uneven mass balance between ingested and excreted CPs at the steady-state that suggest biotransformation of all CPs in the laying hens. Although preliminary studies on this matter have begun to emerge in the literature, knowledge on CPs metabolism is scarce and should be targeted in the near future with dedicated protocols to complete the risk assessment related to the exposure to CPs.

Acknowledgements

The authors acknowledge the French Ministry of Agriculture and Food, General Directorate for Food (DGAl) for its financial support. The authors are grateful to (i) Juliane Glüge and Lena Schinkel for kindly providing the I-42 technical mixture, (ii) to the technical staff of the experimental unit PEAT (INRAE,

Nouzilly, France) and particularly Nicolas Besné and Philippe Didier for the preparation of feed, rearing hens and collecting eggs, (iii) to Thierry Bordeau, Pascal Chartrin and Marie-Dominique Bernadet for their implication in sample collection or preparation, as well as (iv) to Daniela Magalhães for help in sample preparation.

Conflict of interest

The authors declare no financial competing interest.

References

Aamir, M., Yin, S., Zhou, Y., Xu, C., Liu, K., & Liu, W. (2019). Congener-specific C_{10}–C_{13} and C_{14}–C_{17} chlorinated paraffins in Chinese agricultural soils: Spatio-vertical distribution, homologue pattern and environmental behavior. *Environmental Pollution*, *245*, 789–798. https://doi.org/10.1016/j.envpol.2018.10.132

Biessmann, A., Brandt, I., & Darnerud, P. O. (1982). Comparative distribution and metabolism of two ^{14}C-labelled chlorinated paraffins in Japanese quail *Coturnix coturnix japonica*. *Environmental Pollution Series A, Ecological and Biological*, *28*(2), 109–120. https://doi.org/10.1016/0143-1471(82)90097-6

Biessmann, A., Darnerud, P. O., & Brandt, I. (1983). Chlorinated paraffins: Disposition of a highly chlorinated polychlorohexadecane in mice and quail. *Archives of Toxicology*, *53*(1), 79–86. https://doi.org/10.1007/BF01460004

Castro, M., Sobek, A., Yuan, B., & Breitholtz, M. (2019). Bioaccumulation potential of CPs in aquatic organisms: Uptake and depuration in *Daphnia magna*. *Environmental Science & Technology*, *53*, 9533–9541. https://doi.org/10.1021/acs.est.9b01751

Chen, M.-Y., Luo, X.-J., Zhang, X.-L., He, M.-J., Chen, S.-J., & Mai, B.-X. (2011). Chlorinated paraffins in sediments from the Pearl River Delta, South China: Spatial and temporal distributions and

implication for processes. *Environmental Science & Technology*, *45*(23), 9936–9943. https://doi.org/10.1021/es202891a

Conference of the Parties of the Stockholm Convention. (2017). *UNEP/POPS/COP.8/SC.8/11. Listing of short-chain chlorinated paraffins (SCCPs) in Annex A of the Convention* [Web page, accessed on the 4 September 2018]. http://chm.pops.int/TheConvention/ThePOPs/AllPOPs/tabid/2509/Default.aspx

Dong, S., Li, X., Su, X., & Wang, P. (2019). Concentrations and congener group profiles of short- and medium-chain chlorinated paraffins in animal feed materials. *Science of The Total Environment*, *647*, 676–681. https://doi.org/10.1016/j.scitotenv.2018.08.017

European Food Safety Authority (EFSA) panel on contaminants in the food chain (CONTAM). (2020). Risk assessment of chlorinated paraffins in feed and food. *EFSA Journal*, *18*(3), e05991. https://doi.org/10.2903/j.efsa.2020.5991

European Union (EU). (2006). *Regulation (EC) No 1907/2006 of the European Parliament and of the Council of 18 December 2006 concerning the Registration, Evaluation, Authorisation and Restriction of Chemicals (REACH), establishing a European Chemicals Agency, amending Directive 1999/45/EC and repealing Council Regulation (EEC) No 793/93 and Commission Regulation (EC) No 1488/94 as well as Council Directive 76/769/EEC and Commission Directives 91/155/EEC, 93/67/EEC, 93/105/EC and 2000/21/EC* (Official Journal of the European Union). European Union. https://eur-lex.europa.eu/legal-content/EN/ALL/?uri=CELEX:32006R1907

Fisk, A. T., Cymbalisty, C. D., Tomy, G. T., & Muir, D. C. G. (1998). Dietary accumulation and depuration of individual C_{10}-, C_{11}- and C_{11}-polychlorinated alkanes by juvenile rainbow trout (*Oncorhynchus mykiss*). *Aquatic Toxicology*, *43*(2), 209–221. https://doi.org/10.1016/S0166-445X(97)00103-3

Geng, N., Zhang, H., Xing, L., Gao, Y., Zhang, B., Wang, F., Ren, X., & Chen, J. (2016). Toxicokinetics of short-chain chlorinated paraffins in Sprague–Dawley rats following single oral administration. *Chemosphere*, *145*, 106–111. https://doi.org/10.1016/j.chemosphere.2015.11.066

Glüge, J., Wang, Z., Bogdal, C., Scheringer, M., & Hungerbühler, K. (2016). Global production, use, and emission volumes of short-chain chlorinated paraffins - A minimum scenario. *Science of The Total Environment*, *573*, 1132–1146. https://doi.org/10.1016/j.scitotenv.2016.08.105

Government of Canada. (2009). *Toxic substances list: Chlorinated alkanes* [Web page, Accessed on 21 November 2019]. Canada.Ca. https://www.canada.ca/en/environment-climate-change/services/management-toxic-substances/list-canadian-environmental-protection-act/chlorinated-alkanes.html

Harada, K. H., Takasuga, T., Hitomi, T., Wang, P., Matsukami, H., & Koizumi, A. (2011). Dietary exposure to short-chain chlorinated paraffins has increased in Beijing, China. *Environmental Science & Technology*, *45*(16), 7019–7027. https://doi.org/10.1021/es200576d

He, C. (2019). In vitro *biotransformation and identification of potential transformation products of CPs*. 39th edition of the International Symposium on Halogenated Persistent Organic Pollutants, Kyoto, Japan.

International Agency for Research on Cancer (IARC) working group on the evaluation of carcinogenic risk to humans. (1990). Chlorinated Paraffins (Group 2B). In *Some Flame Retardants and Textile Chemicals, and Exposures in the Textile Manufacturing Industry* (Vol. 48, pp. 55–72). https://www.ncbi.nlm.nih.gov/books/NBK519169/

Kan, C. A., & Meijer, G. A. L. (2007). The risk of contamination of food with toxic substances present in animal feed. *Animal Feed Science and Technology*, *133*(1), 84–108. https://doi.org/10.1016/j.anifeedsci.2006.08.005

Krätschmer, K., Malisch, R., Schächtele, A., & Vetter, W. (2019). *Chlorinated paraffins in human milk world-wide: First results from UNEP studies performed between 2012 and 2019*. 39th edition of the International Symposium on Halogenated Persistent Organic Pollutants, Kyoto, Japan.

518 Krätschmer, K., & Schächtele, A. (2019). Interlaboratory studies on chlorinated paraffins: Evaluation
519 of different methods for food matrices. *Chemosphere*, *234*, 252–259.
520 https://doi.org/10.1016/j.chemosphere.2019.06.022
521 Lee, S., Choo, G., Ekpe, O. D., Kim, J., & Oh, J.-E. (2020). Short-chain chlorinated paraffins in various
522 foods from Republic of Korea: Levels, congener patterns, and human dietary exposure.
523 *Environmental Pollution*, *263*, 114520. https://doi.org/10.1016/j.envpol.2020.114520
524 Léon, A., Cariou, R., Hutinet, S., Hurel, J., Guitton, Y., Tixier, C., Munschy, C., Antignac, J.-P., Dervilly-
525 Pinel, G., & Le Bizec, B. (2019). HaloSeeker 1.0: A user-friendly software to highlight
526 halogenated chemicals in nontargeted high-resolution mass spectrometry data sets.
527 *Analytical Chemistry*, *91*(5), 3500–3507. https://doi.org/10.1021/acs.analchem.8b05103
528 Marchand, P., Cariou, R., Vénisseau, A., Brosseaud, A., Antignac, J.-P., & Le Bizec, B. (2010). Predicting
529 PCDD/F and dioxin-like PCB contamination levels in bovine edible tissues from in vivo
530 sampling. *Chemosphere*, *80*(6), 634–640.
531 https://doi.org/10.1016/j.chemosphere.2010.04.057
532 Mézière, M., Cariou, R., Larvor, F., Bichon, E., Guitton, Y., Marchand, P., Dervilly, G., & Bruno, L. B.
533 (2020). Optimized characterization of short-, medium-, and long-chain chlorinated paraffins
534 in liquid chromatography-high resolution mass spectrometry. *Journal of Chromatography A*,
535 *1619*, 460927. https://doi.org/10.1016/j.chroma.2020.460927
536 Mézière, M., Krätschmer, K., Pērkons, I., Zacs, D., Marchand, P., Dervilly, G., Le Bizec, B., Schächtele,
537 A., Cariou, R., & Vetter, W. (2020). Addressing main challenges regarding short- and medium-
538 chain chlorinated paraffin analysis using GC/ECNI-MS and LC/ESI-MS methods. *Journal of the*
539 *American Society for Mass Spectrometry*, *31*, 1885–1895.
540 https://doi.org/10.1021/jasms.0c00155
541 Mézière, M., Marchand, P., Hutinet, S., Larvor, F., Baéza, E., Le Bizec, B., Dervilly, G., & Cariou, R.
542 (2021). Transfer of short-, medium-, and long-chain chlorinated paraffins to eggs of laying

543 hens after dietary exposure. *Food Chemistry, 343, 128491.*
544 *https://doi.org/10.1016/j.foodchem.2020.128491*
545 Niu, S., Chen, R., Zou, Y., Dong, L., Hai, R., & Huang, Y. (2020). Spatial distribution and profile of
546 atmospheric short-chain chlorinated paraffins in the Yangtze River Delta. *Environment*
547 *International*, *259*, 113958. https://doi.org/10.1016/j.envpol.2020.113958
548 Pirard, C., & De Pauw, E. (2005). Uptake of polychlorodibenzo-*p*-dioxins, polychlorodibenzofurans
549 and coplanar polychlorobiphenyls in chickens. *Environment International*, *31*(4), 585–591.
550 https://doi.org/10.1016/j.envint.2004.10.008
551 Pourchet, M., Debrauwer, L., Klanova, J., Price, E. J., Covaci, A., Caballero-Casero, N., Oberacher, H.,
552 Lamoree, M., Damont, A., Fenaille, F., Vlaanderen, J., Meijer, J., Krauss, M., Sarigiannis, D.,
553 Barouki, R., Le Bizec, B., & Antignac, J.-P. (2020). Suspect and non-targeted screening of
554 chemicals of emerging concern for human biomonitoring, environmental health studies and
555 support to risk assessment: From promises to challenges and harmonisation issues.
556 *Environment International*, *139*, 105545. https://doi.org/10.1016/j.envint.2020.105545
557 Rutkowska, M., Płotka-Wasylka, J., Lubinska-Szczygeł, M., Różańska, A., Możejko-Ciesielska, J., &
558 Namieśnik, J. (2018). Birds' feathers - Suitable samples for determination of environmental
559 pollutants. *Trends in Analytical Chemistry*, *109*, 97–115.
560 https://doi.org/10.1016/j.trac.2018.09.022
561 Sun, R., Luo, X., Tang, B., Chen, L., Liu, Y., & Mai, B. (2017). Bioaccumulation of short chain
562 chlorinated paraffins in a typical freshwater food web contaminated by e-waste in south
563 China: Bioaccumulation factors, tissue distribution, and trophic transfer. *Environmental*
564 *Pollution*, *222*, 165–174. https://doi.org/10.1016/j.envpol.2016.12.060
565 Sun, R., Chen, J., Shao, H., Tang, L., Zheng, X., Li, Q. X., Wang, Y., Luo, X., & Mai, B. (2020).
566 Bioaccumulation of short-chain chlorinated paraffins in chicken (*Gallus domesticus*):
567 Comparison to fish. *Journal of Hazardous Materials*, *396*, 122590.
568 https://doi.org/10.1016/j.jhazmat.2020.122590

569 Ueberschär, K.-H., & Matthes, S. (2004). Dose-response feeding study of chlorinated paraffins in
570 broiler chickens: Effects on growth rate and tissue distribution. *Food Additives &*
571 *Contaminants*, *21*(10), 943–948. https://doi.org/10.1080/02652030400006833
572 Ueberschär, K.-H., Dänicke, S., & Matthes, S. (2007). Dose-response feeding study of short chain
573 chlorinated paraffins (SCCPs) in laying hens: Effects on laying performance and tissue
574 distribution, accumulation and elimination kinetics. *Molecular Nutrition & Food Research*,
575 *51*(2), 248–254. https://doi.org/10.1002/mnfr.200600168
576 United States Environmental Protection Agency (US EPA). (2015). *Short-chain chlorinated paraffins*
577 *(SCCPs) and other chlorinated paraffins action plan* [Web page, Accessed on 22 October
578 2019]. US EPA. https://www.epa.gov/assessing-and-managing-chemicals-under-tsca/short-
579 chain-chlorinated-paraffins-sccps-and-other
580 Wang, X., Zhu, J., Xue, Z., Jin, X., Jin, Y., & Fu, Z. (2019). The environmental distribution and toxicity of
581 short-chain chlorinated paraffins and underlying mechanisms: Implications for further
582 toxicological investigation. *The Science of the Total Environment*, *695*, 133834.
583 https://doi.org/10.1016/j.scitotenv.2019.133834
584 Wang, X.-T., Jia, H.-H., Hu, B.-P., Cheng, H.-X., Zhou, Y., & Fu, R. (2019). Occurrence, sources,
585 partitioning and ecological risk of short- and medium-chain chlorinated paraffins in river
586 water and sediments in Shanghai. *Science of The Total Environment*, *653*, 475–484.
587 https://doi.org/10.1016/j.scitotenv.2018.10.391
588 Wang, Y., Gao, W., Wang, Y., & Jiang, G. (2018). Distribution and pattern profiles of chlorinated
589 paraffins in human placenta of Henan province, China. *Environmental Science & Technology*
590 *Letters*, *5*(1), 9–13. https://doi.org/10.1021/acs.estlett.7b00499
591 Yesair, D. W., Callahan, M., Remington, L., & Kensler, C. J. (1970). Role of the entero-hepatic cycle of
592 indomethacin on its metabolism, distribution in tissues and its excretion by rats, dogs and
593 monkeys. *Biochemical Pharmacology*, *19*(5), 1579–1590. https://doi.org/10.1016/0006-
594 2952(70)90146-2

595 Yuan, B., Vorkamp, K., Roos, A. M., Faxneld, S., Sonne, C., Garbus, S. E., Lind, Y., Eulaers, I., Hellström,
596 P., Dietz, R., Persson, S., Bossi, R., & de Wit, C. A. (2019). Accumulation of short-, medium-,
597 and long-chain chlorinated paraffins in marine and terrestrial animals from Scandinavia.
598 *Environmental Science & Technology*, *53*(7), 3526–3537.
599 https://doi.org/10.1021/acs.est.8b06518
600 Zhou, Y., Yin, G., Du, X., Xu, M., Qiu, Y., Ahlqvist, P., Chen, Q., & Zhao, J. (2018). Short-chain
601 chlorinated paraffins (SCCPs) in a freshwater food web from Dianshan Lake: Occurrence
602 level, congener pattern and trophic transfer. *Science of The Total Environment*, *615*, 1010–
603 1018. https://doi.org/10.1016/j.scitotenv.2017.10.026
604
605

606 **Figure captions**

607

608 **Figure 1.** Distribution of the concentrations determined for CP subcategories in laying hen excreta
609 (ng/g dw) and matrices (ng/g lw) at the steady-state. Box plots represent centiles (0, 25, 50, 75 and
610 100). Blue dashed lines represent the LOQ (5 ng/g lw for adipose tissue (AT), liver, muscle, 25 ng/g
611 lw for serum, and 2.5 ng/g dw for excreta).

612

613 **Figure 2.** Daily mass balance of CP subcategories between excreta and egg yolk relative to feed input,
614 estimated over a 14 days period at the steady-state.

615

616 **Figure 3.** 2D-map comparing 95% of the total areas of the CP patterns from day 91 between the
617 collected matrices for exposed laying hens (blue line) or feed (green line) and the exposure mixture
618 (black dashed line).

619

620 **Figure 4.** 3D-representation of the homologue-level accumulation ratios in liver, serum, muscle and
621 adipose tissue after 91 days of exposure.

622

623

Table 1. Accumulation ratios of CP subcategories in laying hen matrices, according to eq. 1.

	SCCPs low %Cl	SCCPs high %Cl	MCCPs	LCCPs low %Cl	LCCPs high %Cl
Egg	0.2*	0.8*/0.3**	0.5*	7.1*	n.c.*
Liver	0.1	0.2/<0.1**	0.4	6.2	3.1
Serum	n.c.	0.6	0.3	7.7	n.c.
Muscle	<0.1	0.1	0.1	0.1	n.c.
Adipose tissue	0.1	0.2/0.5**	0.2	0.1	n.c.

* from Mézière et al. (2021); **from Ueberschär et al. (2007); n.c. : not calculated

Table 2. Parameter *a* of the least-squares approximation with a non-negative constraint, of equation [S] = *a* × [M] + *b*, for the feed and laying hen matrices from the exposed laying hens at day 91 compared to the exposure mixture. Bold: a > 0.7.

	feed	excreta	adipose tissue	carcass	liver	muscle	serum	egg (D89)
SCCPs low %Cl	**1.03**	**1.00**	**0.70**	**0.74**	**0.73**	0.54	n.c.	**0.88***
SCCPs high %Cl	**1.02**	**0.84**	**0.83**	**0.93**	**0.85**	**0.90**	0.53	**1.02***
MCCPs	**1.03**	**0.99**	**0.73**	**0.76**	**0.70**	0.61	0.36	0.57*
LCCPs low %Cl	**1.00**	**0.96**	**0.83**	**0.95**	0.63	n.c.	**0.80**	**0.87***
LCCPs high %Cl	**1.08**	**0.96**	n.c.	n.c.	0.62	n.c.	n.c.	0.52*

n.c.: not calculated, because levels considered as too low; *from Mézière et al. (2021)

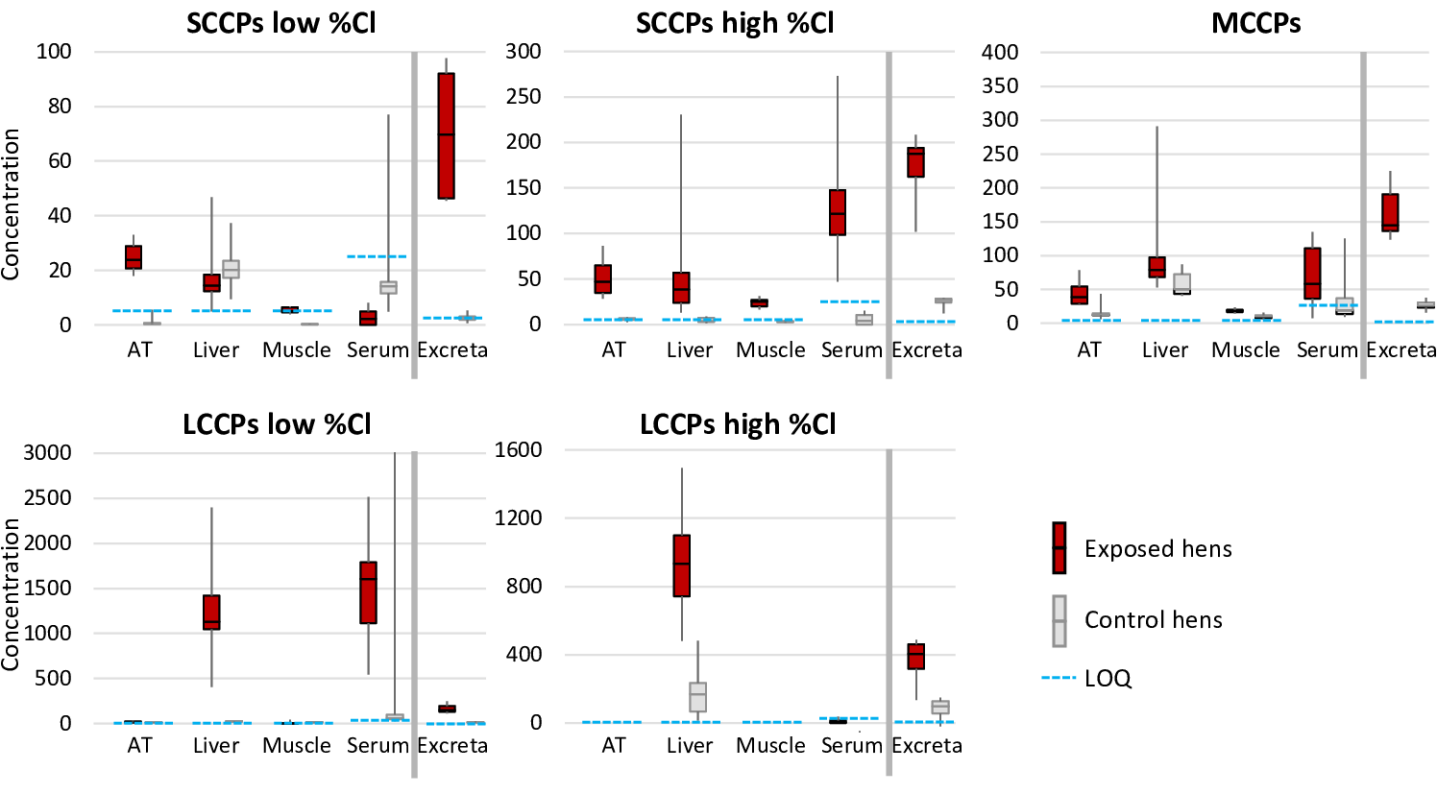
SCCPs low %Cl
SCCPs high %Cl
MCCPs
LCCPs low %Cl
LCCPs high %Cl
Concentration
AT
Liver
Muscle
Serum
Excreta
Exposed hens
Control hens
LOQ

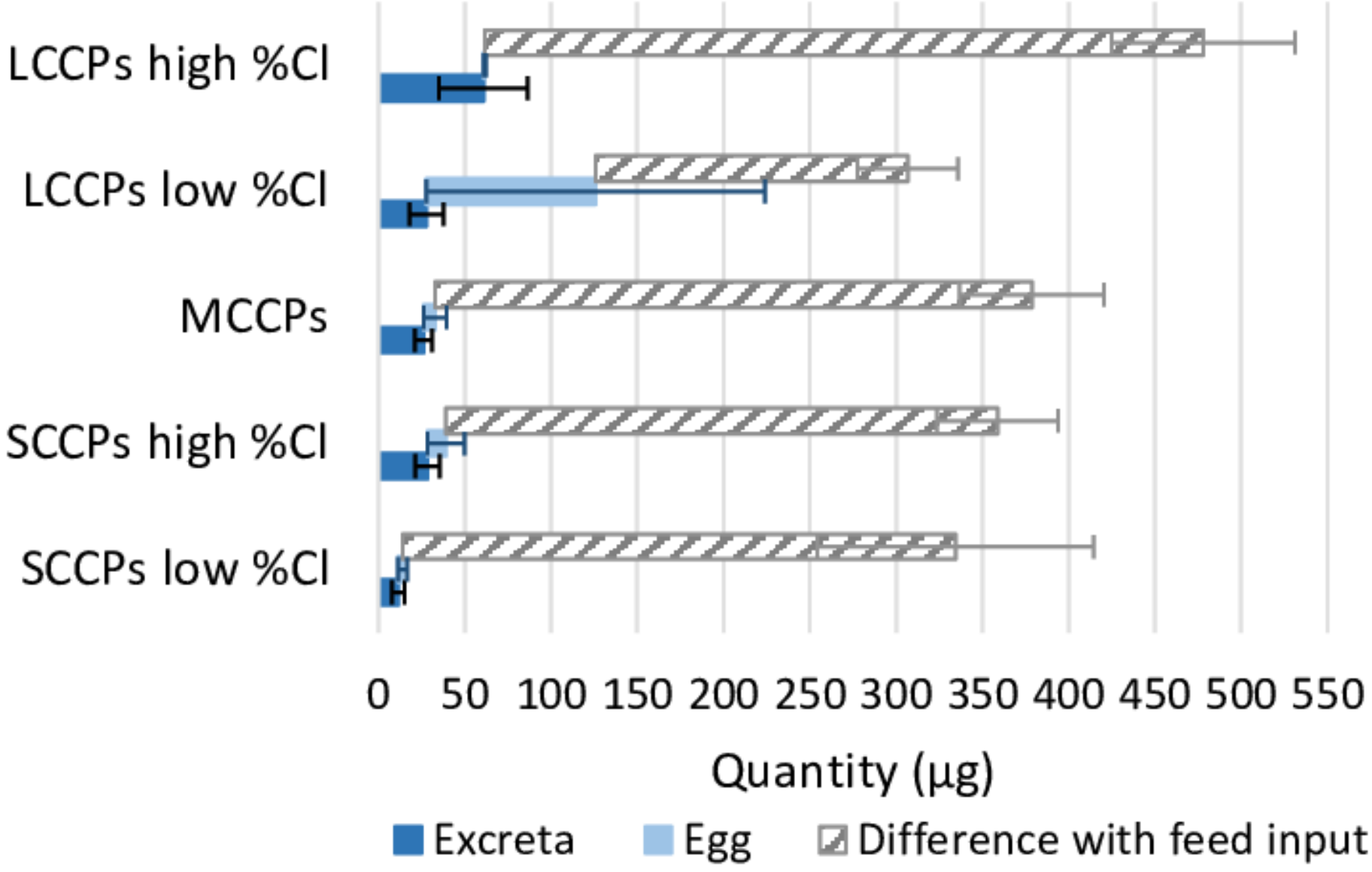
LCCPs high %Cl
LCCPs low %Cl
MCCPs
SCCPs high %Cl
SCCPs low %Cl
0
50
100
150
200
250
300
350
400
450
500
550
Quantity (µg)
Excreta
Egg
Difference with feed input

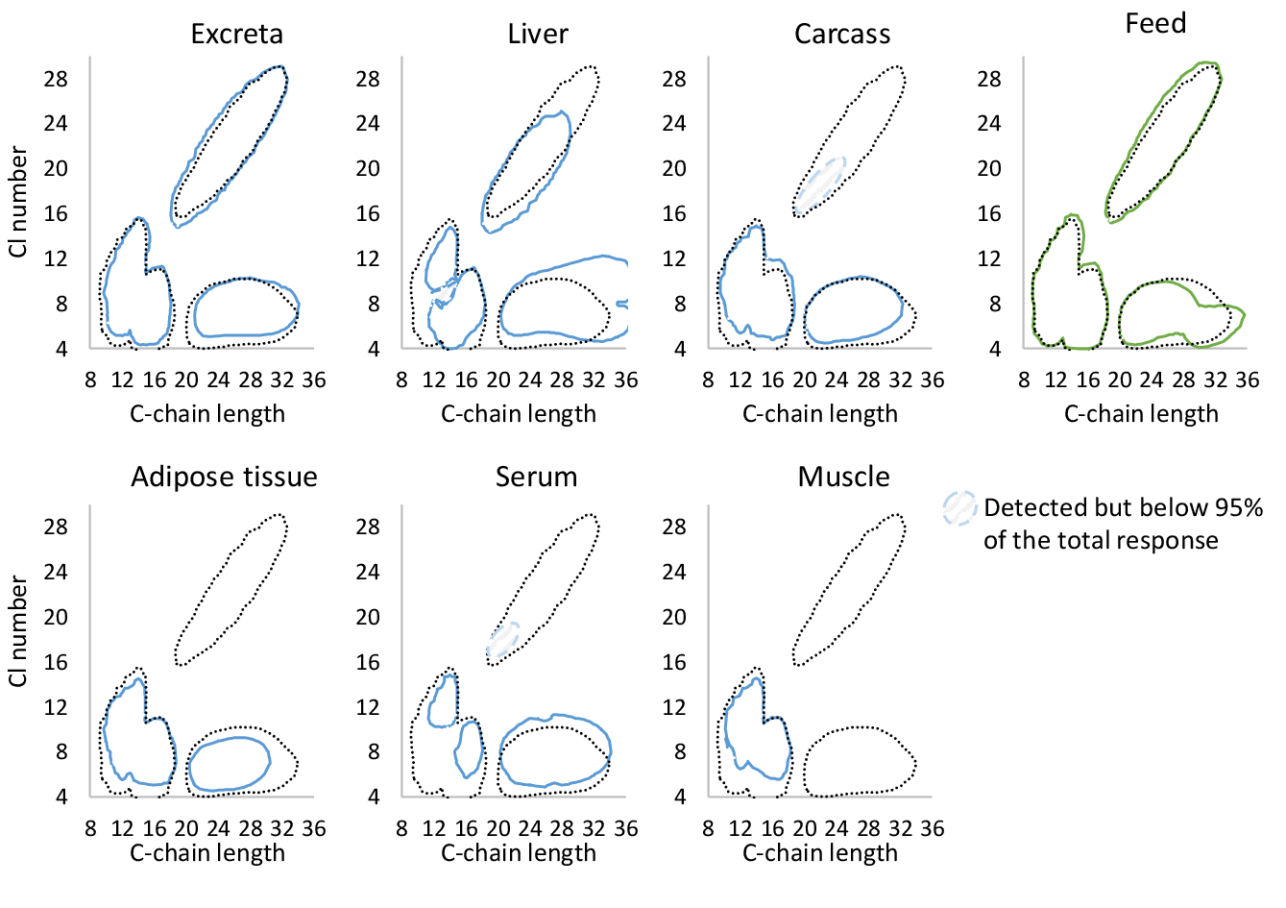
Excreta
Liver
Carcass
Feed
Adipose tissue
Serum
Muscle
Cl number
C-chain length
4
8
12
16
20
24
28
32
36
Detected but below 95% of the total response

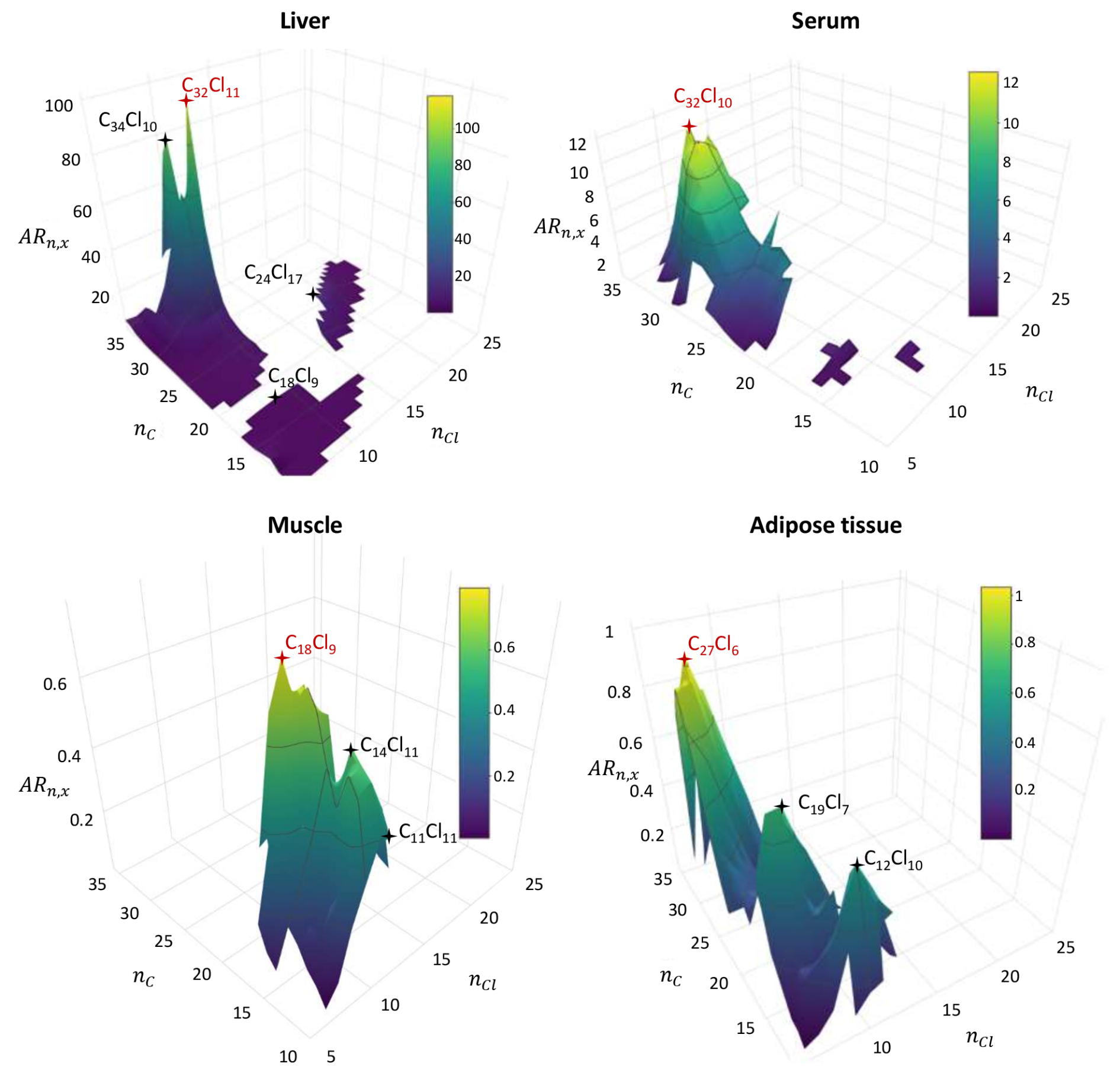
Liver
$C_{32}Cl_{11}$
$C_{34}Cl_{10}$
$C_{24}Cl_{17}$
$C_{18}Cl_9$
$AR_{n,x}$
n_C
n_{Cl}
Serum
$C_{32}Cl_{10}$
$AR_{n,x}$
n_C
n_{Cl}
Muscle
$C_{18}Cl_9$
$C_{14}Cl_{11}$
$C_{11}Cl_{11}$
$AR_{n,x}$
n_C
n_{Cl}
Adipose tissue
$C_{27}Cl_6$
$C_{19}Cl_7$
$C_{12}Cl_{10}$
$AR_{n,x}$
n_C
n_{Cl}